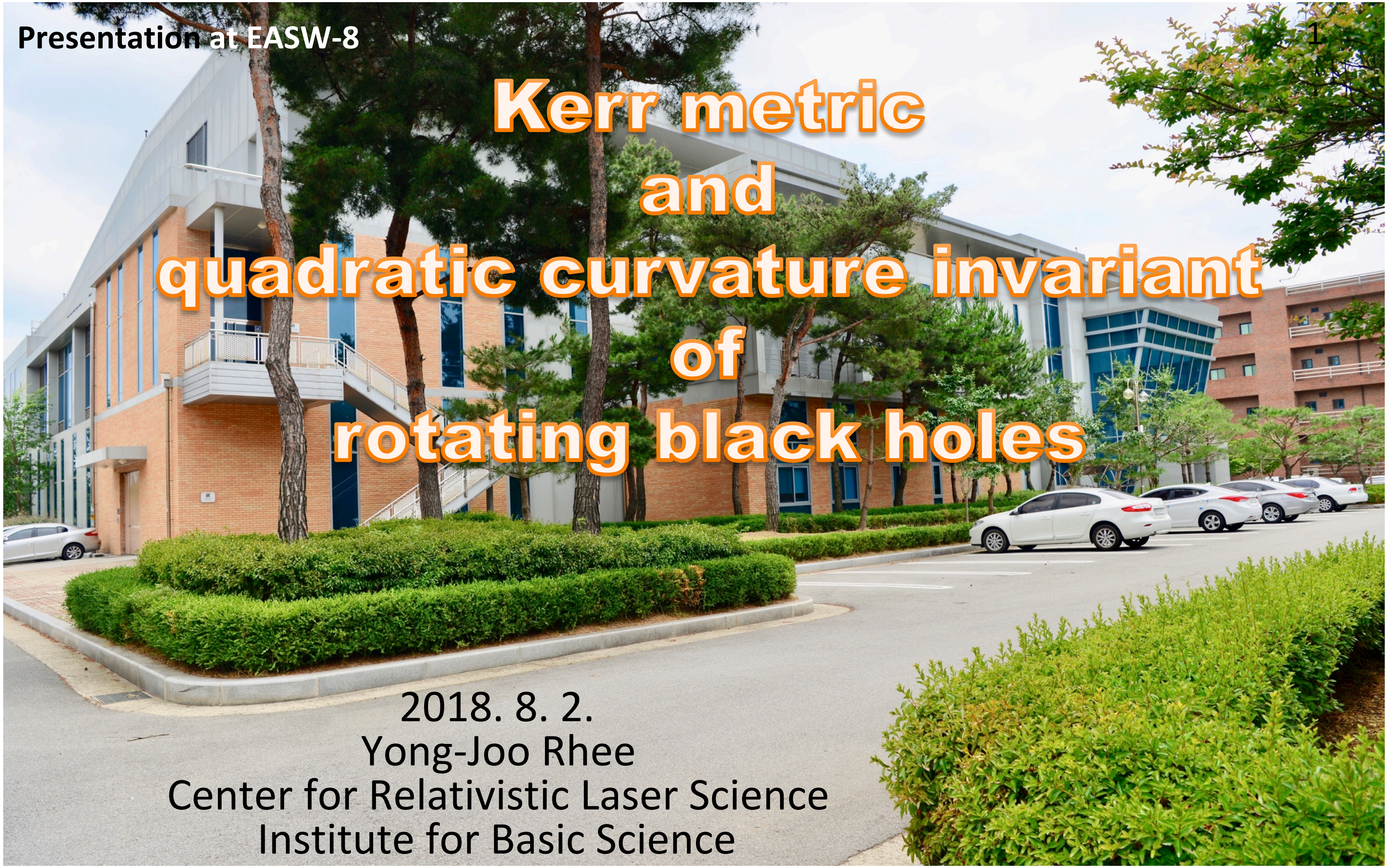

Presentation at EASW-8

Kerr metric and quadratic curvature invariant of rotating black holes

2018. 8. 2.

Yong-Joo Rhee
Center for Relativistic Laser Science
Institute for Basic Science

CONTENTS

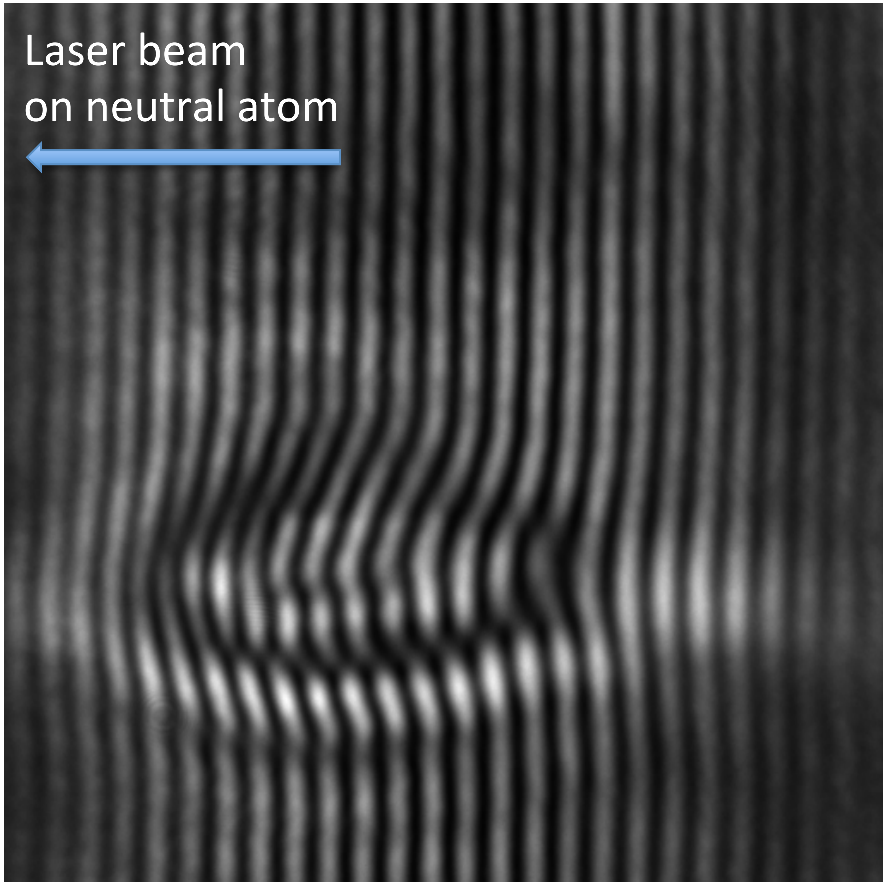

PW interferogram

Ar gas: 10 bar

laser energy: 10 J

1 mm to nozzle (~ 10^{19} − 10^{20} #/cc)

probe delay: 0 mm

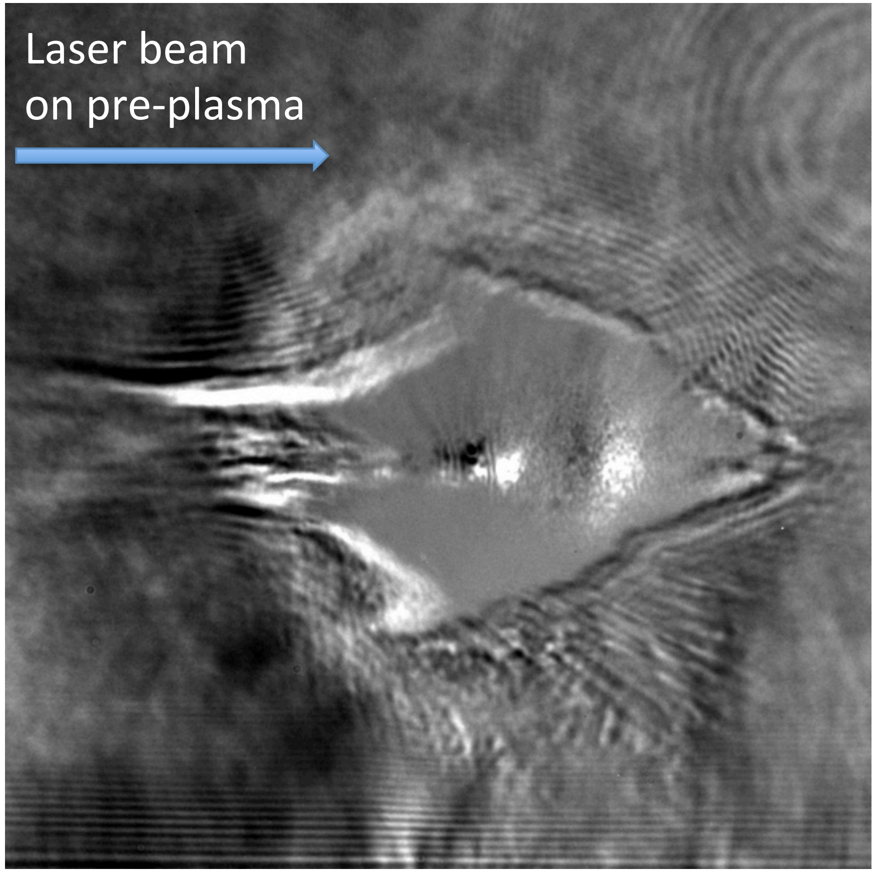

TW shadowgram

Ar gas: 50 bar

Laser energy: 5 J

1 mm to nozzle

probe delay: 67.6 mm

B : 10^6 ~ 10^9 gauss

T_B: a few pico second

Astrophysical jet (wikipedia images)

Spiral galaxy (wikipedia images)

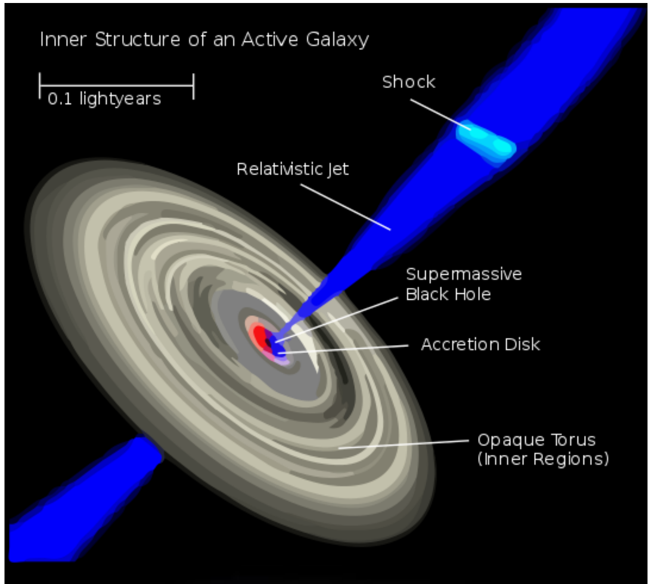

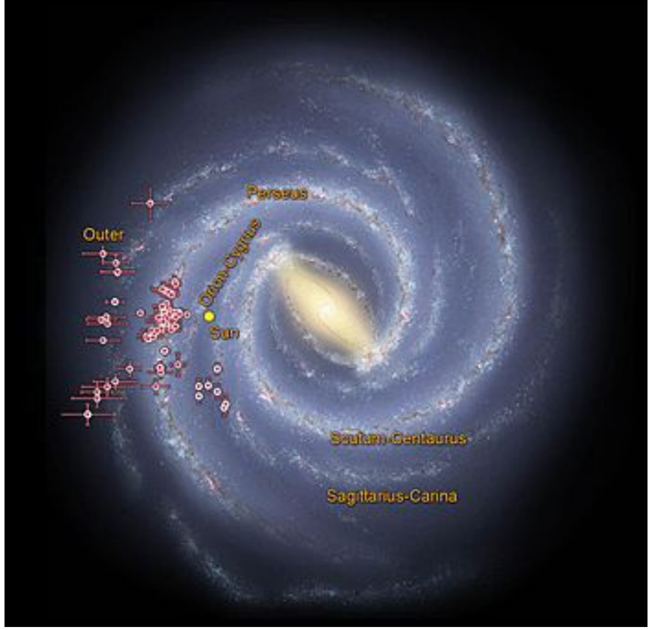

ENERGY SOURCES:

Blandford–Znajek process. This theory explains the extraction of **energy from magnetic fields** around an accretion disk, which are dragged and twisted by the spin of the black hole. Relativistic material is then feasibly launched by the tightening of the field lines.

Penrose mechanism. Here energy is extracted **from a rotating black hole by frame dragging**, which was later theoretically proven to be able to extract relativistic particle energy and momentum, and subsequently shown to be a possible mechanism for jet formation.

https://en.wikipedia.org/wiki/Astrophysical_jet

Since the 1960s, there have been two leading hypotheses or models for the spiral structures of galaxies;
star formation caused by

- **density waves** in the galactic disk of the galaxy
- **shock waves** in the interstellar medium.

(https://en.wikipedia.org/wiki/Spiral_galaxy)

Line elements in Eucledian/Minkowsky space

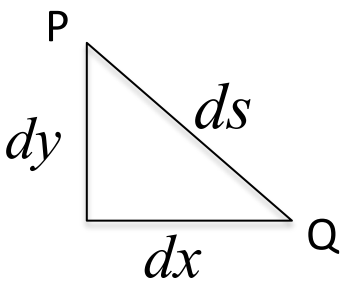

$$ds^2 = dx^2 + dy^2$$

$$ds^2 = dx^2 + dy^2 + dz^2$$

$$ds^2 = dx^2 + dy^2 + dz^2 - c^2 dt^2$$

$$= -c^2 dt^2 + dr^2 + r^2 d\theta^2 + r^2 \sin^2\theta d\phi^2$$

$$\eta = \begin{pmatrix} -c^2 & 0 & 0 & 0 \\ 0 & 1 & 0 & 0 \\ 0 & 0 & 1 & 0 \\ 0 & 0 & 0 & 1 \end{pmatrix}$$

Line elements and a metric tensor in a general space (manifold)

$$ds^2 = g_{\mu\nu}(x) dx^\mu dx^\nu$$

where $g_{\mu\nu}$ is called a metric tensor and characterizes the specific manifold. Superscript is used for contravariant components (dx^μ) and subscript is used for covariant components ($\partial_\mu = \frac{\partial}{\partial x^\mu}$) of tensors.

Metric tensor and magnitude of a vector/tensor

$$g_{\mu\nu}g^{\mu\lambda} = g^{\mu\lambda}g_{\mu\nu} = \delta^{\lambda}_{\nu} \Rightarrow$$ $g_{\mu\nu}$ Is the inverse of $g^{\mu\nu}$

$$|A|^2 = g_{\mu\nu}A^{\mu}A^{\nu} = A_{\mu}A^{\mu} \quad (\neq A^{\mu}A^{\mu}) \Leftarrow \quad A_{\mu} = g_{\mu\nu}A^{\nu}$$

Affine connection

$$\Gamma_{\alpha\beta,\gamma} = \frac{1}{2}\left(\frac{\partial g_{\alpha\gamma}}{\partial x^{\beta}} + \frac{\partial g_{\beta\gamma}}{\partial x^{\alpha}} - \frac{\partial g_{\alpha\beta}}{\partial x^{\gamma}}\right)$$ ← First kind

$$\Gamma^{\gamma}_{\alpha\beta} = g^{\gamma\lambda}\Gamma_{\alpha\beta,\lambda}$$ ← Second kind

$$\frac{1}{2g}\frac{\partial g}{\partial x^{\alpha}} = \Gamma^{\beta}_{\alpha\beta}$$ ← g Is the determinant of $g_{\mu\nu}$

https://en.wikipedia.org/wiki/Affine_connection

In differential geometry, an affine connection is a geometric object on a smooth manifold which connects nearby tangent spaces, and so permits tangent vector fields to be differentiated as if they were functions on the manifold with values in a fixed vector space

Covariant derivative

$$D_\alpha A_\beta = \partial_\alpha A_\beta - \Gamma^{\gamma}_{\beta\alpha} A_\gamma$$

$$D_\alpha A^\beta = \partial_\alpha A^\beta - \Gamma^{\beta}_{\gamma\alpha} A^\gamma$$

$$D_\gamma g_{\alpha\beta} = 0 \quad D_\gamma g^{\alpha\beta} = 0 \quad D_\gamma \delta^{\beta}_{\alpha} = 0$$

$D_\gamma f = \partial_\gamma f$ (for a scalar field f)

$D_\alpha A_\beta$ is a tensor of 2nd rank whereas $\partial_\alpha A_\beta$ is not a tensor since it does not follow the tensorial transformation properties under coordinate transformation.

Riemannian curvature tensor and torsion tensor

$$\begin{aligned}
&\left(D_\alpha D_\beta - D_\beta D_\alpha\right) A_\gamma \\
&= \left(\partial_\beta \Gamma^{\eta}_{\gamma\alpha} - \partial_\alpha \Gamma^{\eta}_{\gamma\beta} + \Gamma^{\varepsilon}_{\gamma\alpha}\Gamma^{\eta}_{\varepsilon\beta} - \Gamma^{\varepsilon}_{\gamma\beta}\Gamma^{\eta}_{\varepsilon\alpha}\right) A_\eta + \left(\Gamma^{\delta}_{\alpha\beta} - \Gamma^{\delta}_{\beta\alpha}\right) D_\delta A_\gamma \\
&= R^{\eta}_{\gamma\,\alpha\beta} A_\eta + S^{\delta}_{\alpha\beta} D_\delta A_\gamma
\end{aligned}$$

Ricci curvature tensor and Einstein's field equation

$$R_{\alpha\beta} = R_{\alpha\ \beta\eta}^{\ \eta} = g^{\varepsilon\eta} R_{\alpha\varepsilon\beta\eta}$$

$$D_\alpha \left(R^\alpha_{\ \beta} - \frac{1}{2}\delta^\alpha_{\ \beta} R \right) = 0 \qquad R = g^{\alpha\beta} R_{\alpha\beta} \qquad (R \text{ : scalar curvature})$$

$$G^\alpha_{\ \beta} \equiv R^\alpha_{\ \beta} - \frac{1}{2}\delta^\alpha_{\ \beta} R \qquad \text{(Einstein tensor)}$$

$$\Rightarrow D_\alpha G^\alpha_{\ \beta} = 0 \qquad \text{(Divergence of Einstein tensor vanishes)}$$

$$\boxed{R_{\alpha\beta} - \frac{1}{2} R g_{\alpha\beta} + \Lambda g_{\alpha\beta} = \frac{8\pi G}{c^4} T_{\alpha\beta}}$$

G is the Newton's gravitational constant, T represents the matter distribution, Λ is the cosmological constant. Thus the geometrical field g is determined by the matter tensor T.

Exact solutions of Einstein's field equation

	Non-rotating (J = 0)	**Rotating (J ≠ 0)**
Uncharged (Q=0)	Schwarzschild (1915)	Kerr (1963)
Charged (Q ≠ 0)	Reissner-Nordstrom (1916-1918)	Kerr-Newman (1965)

For spherically symmetric and stationary system, the solution is Schwarzschild solution;

$$ds^2 = -\left(1-\frac{a}{r}\right)c^2dt^2 + \left(1-\frac{a}{r}\right)^{-1}dr^2 + r^2 d\theta^2 + r^2\sin^2\theta d\phi^2$$

where a is the Schwarzschild radius. $\left(a = \dfrac{2Gm}{c^2}\right)$

$$\boxed{\begin{aligned} a_\odot &\approx 3km \\ a_E &\approx 9mm \end{aligned}}$$

For a spherically symmetric rotating system with an angular momentum J, the equation is solved in Boyer-Lyndquist coordinates;

$$ds^2 = -\left[1 - \frac{ar}{r^2 + b^2\cos^2\theta}\right]c^2dt^2 - \frac{2abr\sin^2\theta}{r^2 + b^2\cos^2\theta}cdtd\phi + \left[\frac{r^2 + b^2\cos^2\theta}{r^2 - ar + b^2}\right]dr^2$$

$$+\left(r^2 + b^2\cos^2\theta\right)d\theta^2 + \left[r^2 + b^2 + \frac{ab^2r\sin^2\theta}{r^2 + b^2\cos^2\theta}\right]\sin^2\theta\, d\phi^2$$

$$a = {2Gm}/{c^2}$$

$$b = {J}/{mc}$$

$$\chi = \cos\theta \qquad d\chi = \sin\theta d\theta \qquad \chi \in \left[-1,\ 1\right]$$

$$ds^2 = -\left\{1 - \frac{ar}{r^2 + b^2\chi^2}\right\}c^2dt^2 - \frac{2abr\left(1-\chi^2\right)}{r^2 + b^2\chi^2}cdtd\phi + \frac{r^2 + b^2\chi^2}{r^2 - ar + b^2}dr^2$$

$$+\frac{r^2 + b^2\chi^2}{1-\chi^2}d\chi^2 + \left(1-\chi^2\right)\left\{r^2 + b^2 + \frac{ab^2r\left(1-\chi^2\right)}{r^2 + b^2\chi^2}\right\}d\phi^2$$

$$g_{\alpha\beta} = \begin{bmatrix} -1+\dfrac{ar}{r^2+b^2\chi^2} & 0 & 0 & -\dfrac{abr\left(1-\chi^2\right)}{r^2+b^2\chi^2} \\ 0 & \dfrac{r^2+b^2\chi^2}{r^2-ar+b^2} & 0 & 0 \\ 0 & 0 & \dfrac{r^2+b^2\chi^2}{1-\chi^2} & 0 \\ -\dfrac{abr\left(1-\chi^2\right)}{r^2+b^2\chi^2} & 0 & 0 & \left(1-\chi^2\right)\left\{r^2+b^2+\dfrac{ab^2r\left(1-\chi^2\right)}{r^2+b^2\chi^2}\right\} \end{bmatrix}$$

Quadratic curvature invariant (Kretschmann scalar)

$$K = R^{\alpha\beta\gamma\delta}R_{\alpha\beta\gamma\delta} = \frac{12a^2\left(r^2-b^2\chi^2\right)\left[\left(r^2+b^2\chi^2\right)^2-16r^2b^2\chi^2\right]}{\left(r^2+b^2\chi^2\right)^6}$$

Singularities and surfaces

$$r^2 + b^2\chi^2 = 0 \ \rightarrow r = 0 \ and \ \chi = 0 \ (\theta = \pi / 2)$$

curvature singularity $(x^2 + y^2 = b^2 \ and \ z = 0)$

$$r^2 - ar + b^2 = 0 \ \rightarrow \ r_{\pm} = \frac{a \pm \sqrt{a^2 - 4b^2}}{2}$$

event horizons

$$r^2 - ar + b^2\chi^2 = 0 \ \rightarrow \ r_{\pm}^{E} = \frac{a \pm \sqrt{a^2 - 4b^2\chi^2}}{2}$$

ergosphere → frame dragging

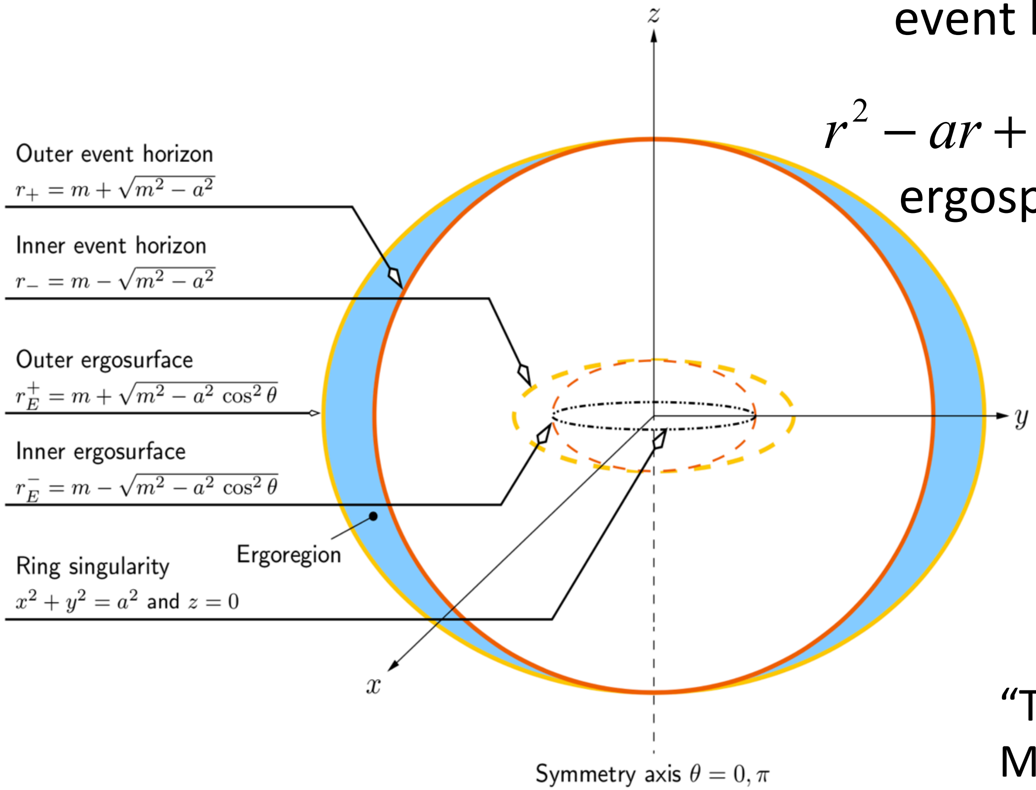

$a = 2Gm/c^2$ Schwarzschild radius

$b = J/mc$ angular momentum

"The Kerr spacetime: A brief introduction"
Matt Visser, arXiv:0706.0622v3 (15 Jan 2008)

Plot of quadratic curvature invariant

In[6]:=
```
Manipulate[
 Plot3D[
  -((24 a^2 (10 b^6 - 180 b^4 r^2 + 240 b^2 r^4 - 32 r^6 +
         15 b^2 (b^4 - 16 b^2 r^2 + 16 r^4) Cos[2 θ] +
         6 b^4 (b^2 - 10 r^2) Cos[4 θ] + b^6 Cos[6 θ])) /
     (b^2 + 2 r^2 + b^2 Cos[2 θ])^6), {r, -2, 2}, {θ, Pi, 0},
  PlotRange → {-10, 10}], {a, 0, 2}, { b, 0, 3}]
```

Out[6]=

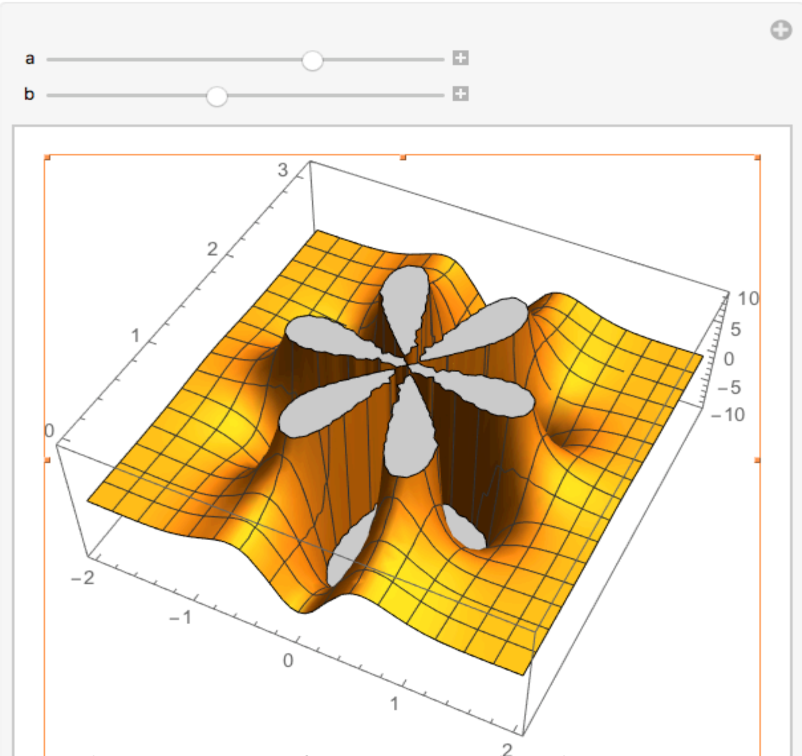

Leonard Parker, University of Wisconsin, Milwaukee

Contour plot of quadratic curvature invariant

In[7]:=
```
Manipulate[
 ContourPlot[
  -((24 a^2 (10 b^6 - 180 b^4 r^2 + 240 b^2 r^4 - 32 r^6 +
         15 b^2 (b^4 - 16 b^2 r^2 + 16 r^4) Cos[2 θ] +
         6 b^4 (b^2 - 10 r^2) Cos[4 θ] + b^6 Cos[6 θ])) /
     (b^2 + 2 r^2 + b^2 Cos[2 θ])^6), {r, -2, 2}, {θ, Pi, 0},
  PlotRange → {-10, 10}, Contours → 10], {a, 0, 2},
 {b, 0, 3}]
```

Out[7]=

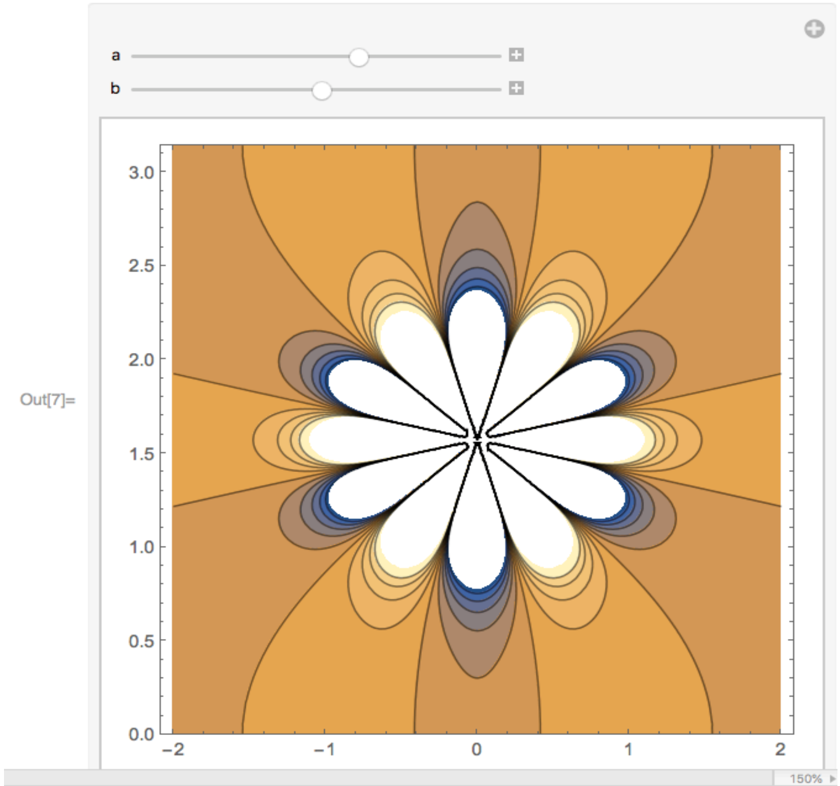

THE ASTROPHYSICAL JOURNAL, 535:350–353, 2000 May 20

KRETSCHMANN SCALAR FOR A KERR-NEWMAN BLACK HOLE

RICHARD CONN HENRY
Center for Astrophysical Sciences, Department of Physics and Astronomy, The Johns Hopkins University, Baltimore, MD 21218-2686; henry@jhu.edu
Received 1999 June 11; accepted 2000 January 11

ABSTRACT

I have derived the Kretschmann scalar for a general black hole of mass *m*, angular momentum per unit mass *a*, and electric charge *Q*. The Kretschmann scalar gives the amount of curvature of spacetime, as a function of position near (and within) a black hole. This allows one to display the "appearance" of the black hole *itself*, whether the black hole is merely of stellar mass or is a supermassive black hole at the center of an active galaxy. Schwarzschild black holes, rotating black holes, electrically charged black holes, and rotating electrically charged black holes are all illustrated. Rotating black holes are discovered to possess a negative curvature that is *not* analogous to that of a saddle.

FORTRAN code
\+ Mathematica
→ 1.3 MB of script text file for input to Mathematica 2.2

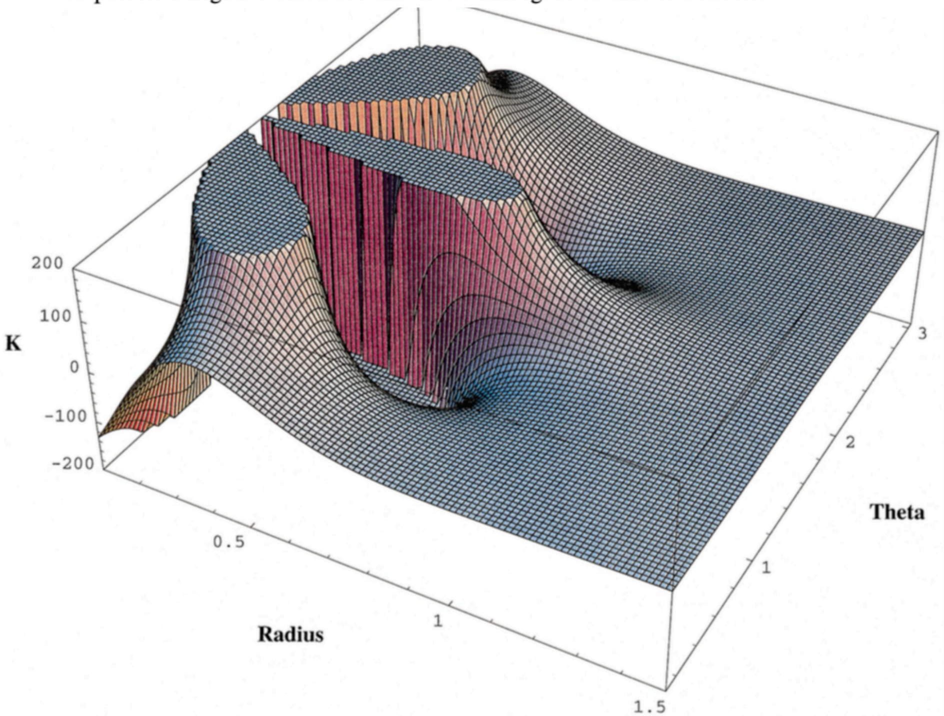

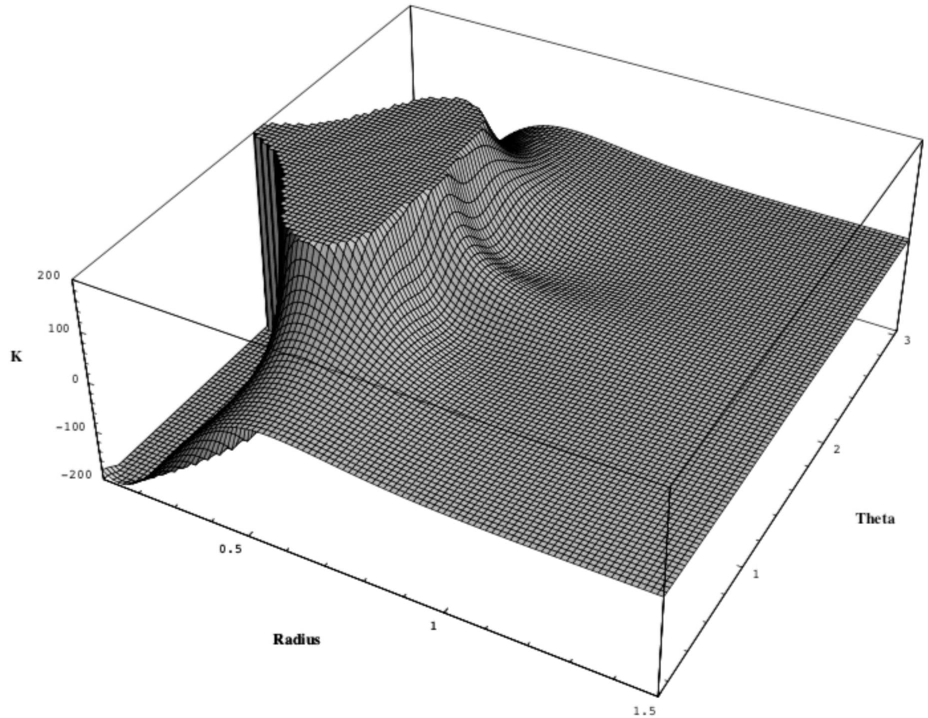

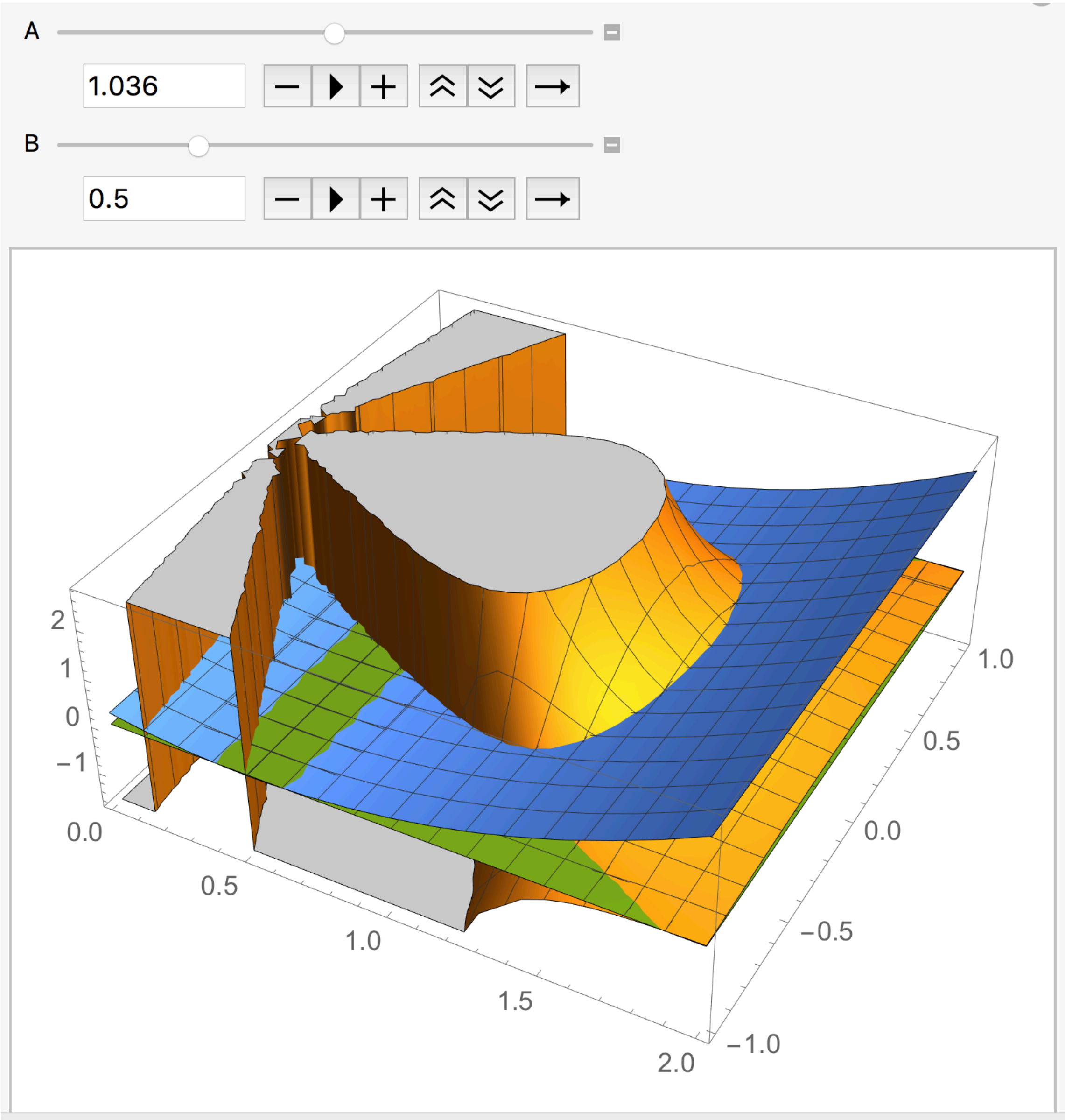

Orange:

quadratic curvature invariant (Kretschmann scalar)

Blue:

coordinate singularity if zero (event horizon: inner, outer)

Green:

zero curvature invariant plane

For a Schwarzschild black hole of mass M, the Kretschmann scalar is[1]

$$K = \frac{48 G^2 M^2}{c^4 r^6} .$$

where G is the gravitational constant.

For a de Sitter or Anti de Sitter metric

$$ds^2 = -\mathrm{d}t^2 + e^{2Ht}\left(\frac{\mathrm{d}r^2}{1-kr^2} + r^2\mathrm{d}\theta^2 + r^2\sin^2\theta\mathrm{d}\phi^2\right),$$

the Kretschmann scalar is

$$K = 24H^4 .$$

For a general FRW spacetime with metric

$$ds^2 = -\mathrm{d}t^2 + a(t)^2\left(\frac{\mathrm{d}r^2}{1-kr^2} + r^2\mathrm{d}\theta^2 + r^2\sin^2\theta\mathrm{d}\phi^2\right),$$

the Kretschmann scalar is

$$K = \frac{12\left(a(t)^2 a''(t)^2 + \left(k - a'(t)^2\right)^2\right)}{a(t)^4} .$$

The Astrophysical Journal Letters, 731:L5 (5pp), 2011 April 10 doi:10.1088/2041-8205/731/1/L5

THE ANGULAR MOMENTA OF NEUTRON STARS AND BLACK HOLES AS A WINDOW ON SUPERNOVAE

J. M. Miller[1], M. C. Miller[2], and C. S. Reynolds[2]
[1] Department of Astronomy, University of Michigan, 500 Church Street, Ann Arbor, MI 48109-1042, USA; jonmm@umich.edu
[2] Department of Astronomy, University of Maryland, College Park, MD 20742, USA
Received 2010 December 20; accepted 2011 February 7; published 2011 March 17

ABSTRACT

It is now clear that a subset of supernovae displays evidence for jets and is observed as gamma-ray bursts (GRBs). The angular momentum distribution of massive stellar endpoints provides a rare means of constraining the nature of the central engine in core-collapse explosions. Unlike supermassive black holes, the spin of stellar-mass black holes in X-ray binary systems is little affected by accretion and accurately reflects the spin set at birth. A modest number of stellar-mass black hole angular momenta have now been measured using two independent X-ray spectroscopic techniques. In contrast, rotation-powered pulsars spin down over time, via magnetic braking, but a modest number of natal spin periods have now been estimated. For both canonical and extreme neutron star parameters, statistical tests strongly suggest that the angular momentum distributions of black holes and neutron stars are markedly different. Within the context of prevalent models for core-collapse supernovae, the angular momentum distributions are consistent with black holes typically being produced in GRB-like supernovae with jets and with neutron stars typically being produced in supernovae with too little angular momentum to produce jets via magnetohydrodynamic processes. It is possible that neutron stars are with high spin initially and rapidly spun down shortly after the supernova event, but the available mechanisms may be inconsistent with some observed pulsar properties.

Key words: accretion, accretion disks – black hole physics – gamma-ray burst: general – stars: evolution – stars: neutron – supernovae: general

Table 1
Black Hole Angular Momenta

Source	cJ/GM^2 (reflection) $\left(= 2b/a\right)$	cJ/GM^2 (continuum)
M33 X-7	...	0.77(5)[a]
LMC X-1	...	0.92(6)[b]
A 0620−00	...	0.12(19)[c]
4U 1543−475	0.3(1)[d]	0.80(5)[e]
XTE J1550−564	0.76(1)[d]	...
XTE J1650−500	0.79(1)[d]	...
XTE J1652−453	0.45(2)[f]	...
GRO J1655−40	0.98(1)[d]	0.70(5)[e]
GX 339−4	0.94(2)[d]	...
SAX J1711.6−3808	0.6(3)[d]	...
XTE J1752−223	0.55(11)[g]	...
Swift J1753.5−0127	0.76(13)[h]	...
XTE J1908+094	0.75(9)[d]	...
GRS 1915+105	0.98(1)[i]	0.99(1)[j]
Cygnus X-1	0.05(1)[d]	...

Notes. Measured values of black hole spin parameters are given above. The errors are statistical errors on the last significant digit.

References. [a] Liu et al. 2008; [b] Gou et al. 2009; [c] Gou et al. 2010; [d] Miller et al. 2009; [e] Shafee et al. 2006; [f] Hiemstra et al. 2011; [g] Reis et al. 2011; [h] Reis et al. 2009; [i] Blum et al. 2009; [j] McClintock et al. 2006.

Table 2
Distribution Properties

Sample	a_{mean}	a_{median}
BH (reflection)	0.66	0.76
BH (continuum)	0.72	0.80
NS (natal; 1.4 $M_\odot$, R = 15 km)	0.029	0.017
NS (natal; 1.4 $M_\odot$, R = 10 km)	0.018	0.007

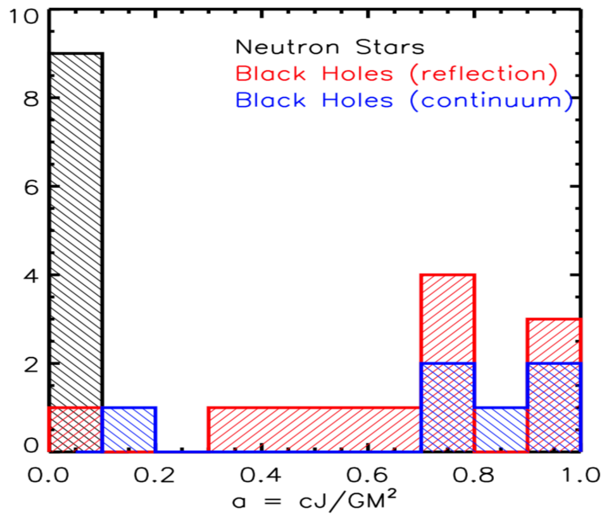

Figure 1. Distribution of dimensionless angular momenta for neutron stars and stellar-mass black holes, compiled from recent measurements, is shown here. The neutron star momenta were calculated using the subset of rotation-powered pulsars wherein natal spin periods have been estimated. Stellar radii of 15 km and masses of 1.4 $M_\odot$ were assumed in all cases in order to give the greatest possible angular momentum values. A two-sided Kolmogorov-Smirnov test was used to evaluate the probability that neutron star and black hole spins were drawn from the same parent distribution. A probability of 3.6×10^{-4} is found when comparing neutron star spins to black hole spins derived using the disk continuum. The probability is 9.3×10^{-5} when using black hole spins derived using disk reflection.

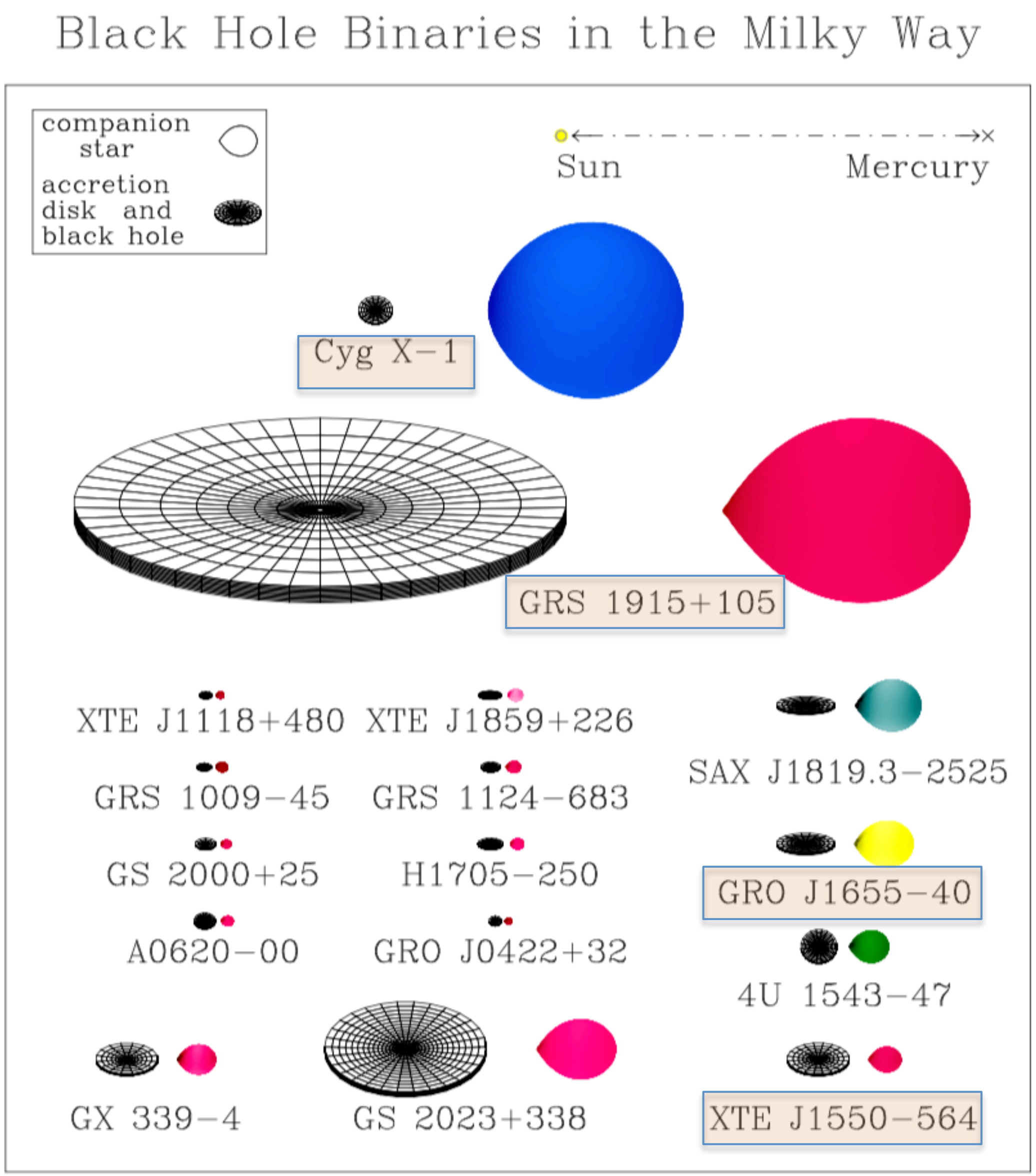

X-ray Properties of Black-Hole Binaries

Ronald A. Remillard (MIT Kavli Institute), Jeffrey E. McClintock (Harvard-Smithsonian Center for Astrophysics)

(Submitted on 14 Jun 2006)

We review the properties and behavior X-ray binaries that contain an accreting black hole. The larger majority of such systems are X-ray transients, and many of them were observed in daily pointings with RXTE throughout the course of their outbursts. The complex evolution of these sources is described in terms of common behavior patterns illustrated with comprehensive overview diagrams for six selected systems. Central to this comparison are three X-ray states of accretion, which are reviewed and defined quantitatively. Each state yields phenomena that arise in strong gravitational fields. We sketch a scenario for the potential impact of black hole observations on physics and discuss a current frontier topic: the measurement of black hole spin.

Comments:	39 pages, 12 figures, ARAA, vol. 44, in press
Subjects:	**Astrophysics (astro-ph)**
Journal reference:	Ann.Rev.Astron.Astrophys.44:49-92,2006

Figure 1: Scale drawings of 16 black-hole binaries in the Milky Way (courtesy of J. Orosz). The Sun–Mercury distance (0.4 AU) is shown at the top. The estimated binary inclination is indicated by the tilt of the accretion disk. The color of the companion star roughly indicates its surface temperature.

Table 1: Twenty confirmed black holes and twenty black hole candidates[a]

Coordinate Name	Common[b] Name/Prefix	Year[c]	Spec.	P_{orb} (hr)	f(M) ($M_\odot$)	M_1 ($M_\odot$)
0422+32	(GRO J)	1992/1	M2V	5.1	1.19±0.02	3.7–5.0
0538–641	LMC X–3	–	B3V	40.9	2.3±0.3	5.9–9.2
0540–697	LMC X–1	–	O7III	93.8[d]	0.13±0.05[d]	4.0–10.0:[e]
0620–003	(A)	1975/1[f]	K4V	7.8	2.72±0.06	8.7–12.9
1009–45	(GRS)	1993/1	K7/M0V	6.8	3.17±0.12	3.6–4.7:[e]
1118+480	(XTE J)	2000/2	K5/M0V	4.1	6.1±0.3	6.5–7.2
1124–684	Nova Mus 91	1991/1	K3/K5V	10.4	3.01±0.15	6.5–8.2
1354–64[g]	(GS)	1987/2	GIV	61.1[g]	5.75±0.30	–
1543–475	(4U)	1971/4	A2V	26.8	0.25±0.01	8.4–10.4
1550–564	(XTE J)	1998/5	G8/K8IV	37.0	6.86±0.71	8.4–10.8
1650–500[h]	(XTE J)	2001/1	K4V	7.7	2.73±0.56	–
1655–40	(GRO J)	1994/3	F3/F5IV	62.9	2.73±0.09	6.0–6.6
1659–487	GX 339–4	1972/10[i]	–	42.1[j,k]	5.8±0.5	–
1705–250	Nova Oph 77	1977/1	K3/7V	12.5	4.86±0.13	5.6–8.3
1819.3–2525	V4641 Sgr	1999/4	B9III	67.6	3.13±0.13	6.8–7.4
1859+226	(XTE J)	1999/1	–	9.2:[e]	7.4±1.1:[e]	7.6–12.0:[e]
1915+105	(GRS)	1992/Q[l]	K/MIII	804.0	9.5±3.0	10.0–18.0
1956+350	Cyg X–1	–	O9.7Iab	134.4	0.244±0.005	6.8–13.3
2000+251	(GS)	1988/1	K3/K7V	8.3	5.01±0.12	7.1–7.8
2023+338	V404 Cyg	1989/1[f]	K0III	155.3	6.08±0.06	10.1–13.4

GRO J1655-40
A = 6.3
S = 0.98
Q =0

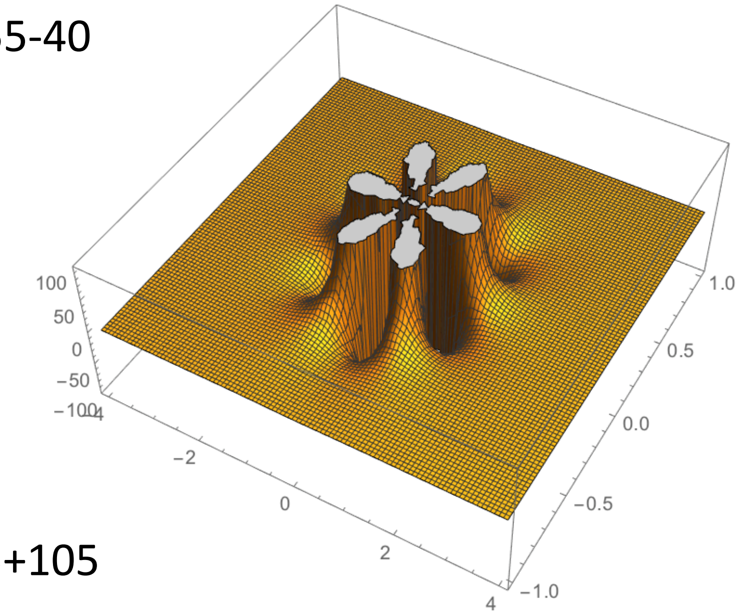

XTE J1550-564
A = 9.6
S = 0.76
Q = 0

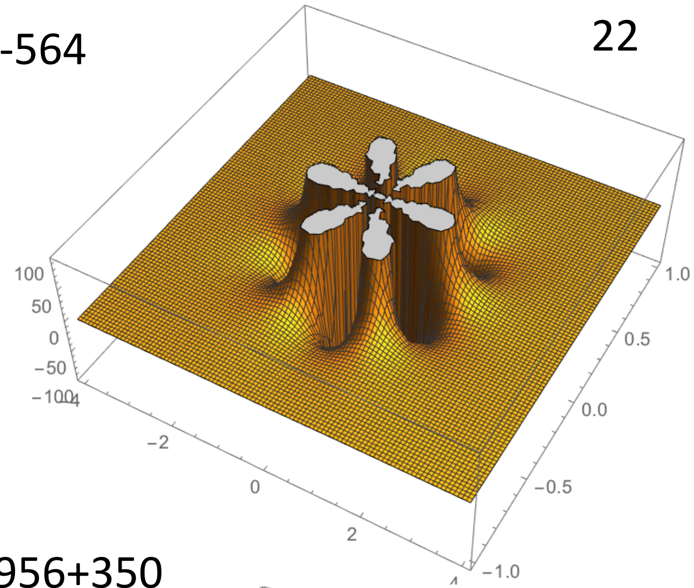

GRS 1915+105
A = 14
S = 0.98
Q =0

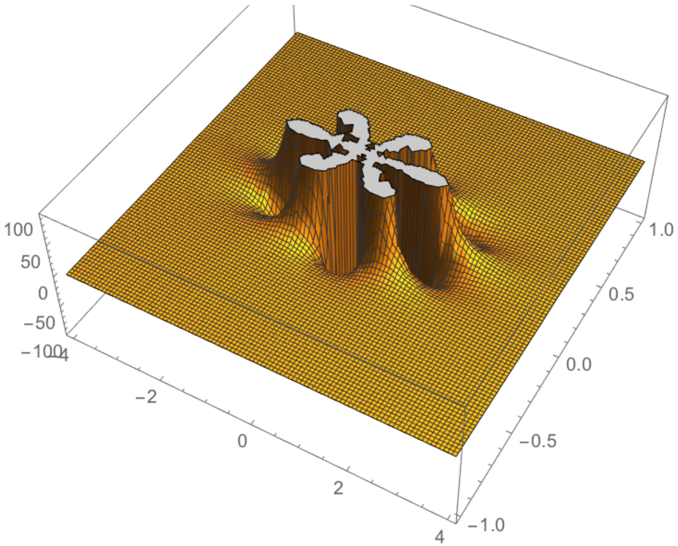

CYG X-1 1956+350
A = 10
S = 0.05
Q =0

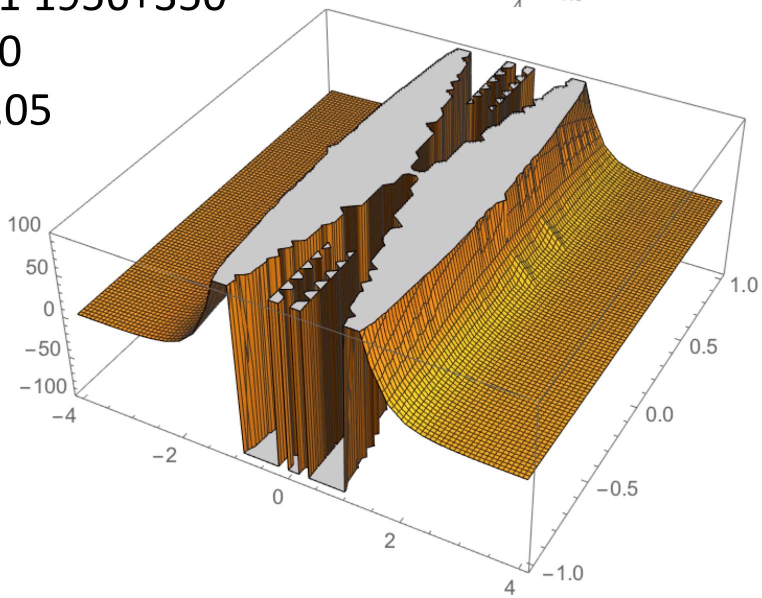

GRO J1655-40
A = 6.3
S = 0.98
Q =0

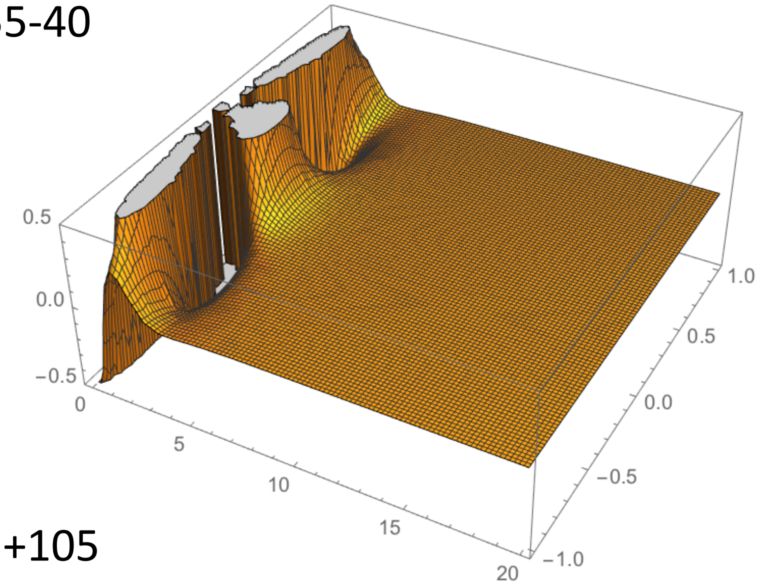

XTE J1550-564
A = 9.6
S = 0.76
Q = 0

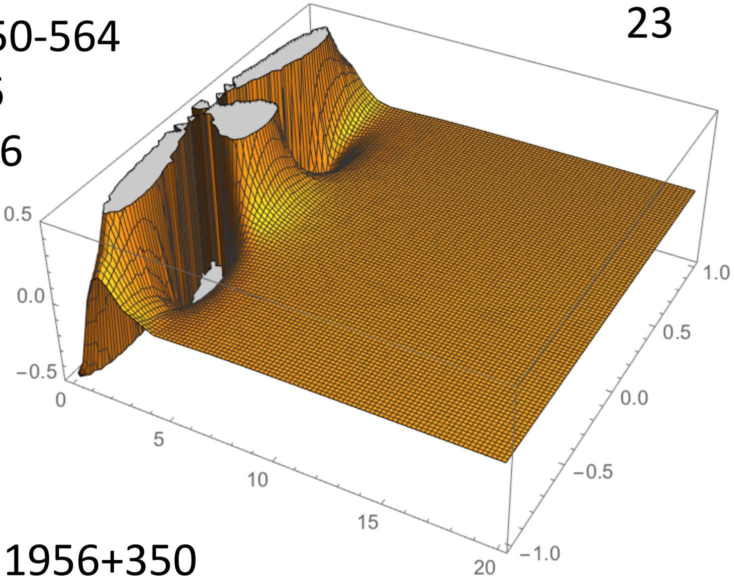

GRS 1915+105
A = 14
S = 0.98
Q =0

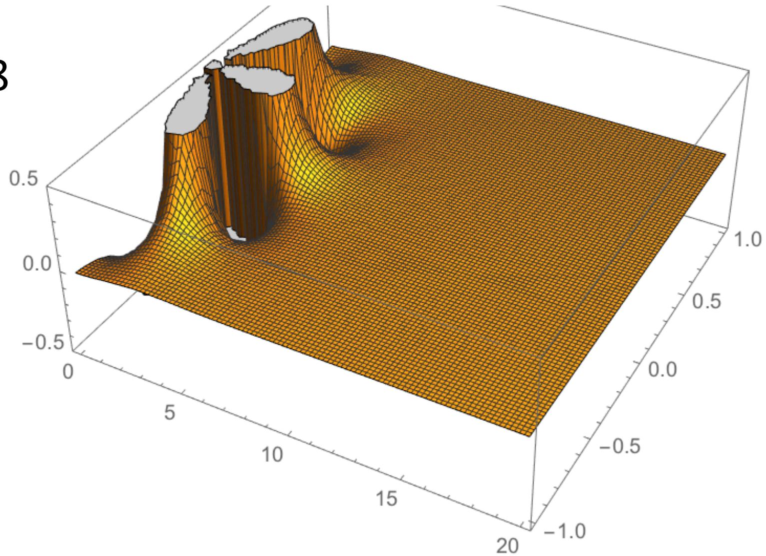

CYG X-1 1956+350
A = 10
S = 0.05
Q =0

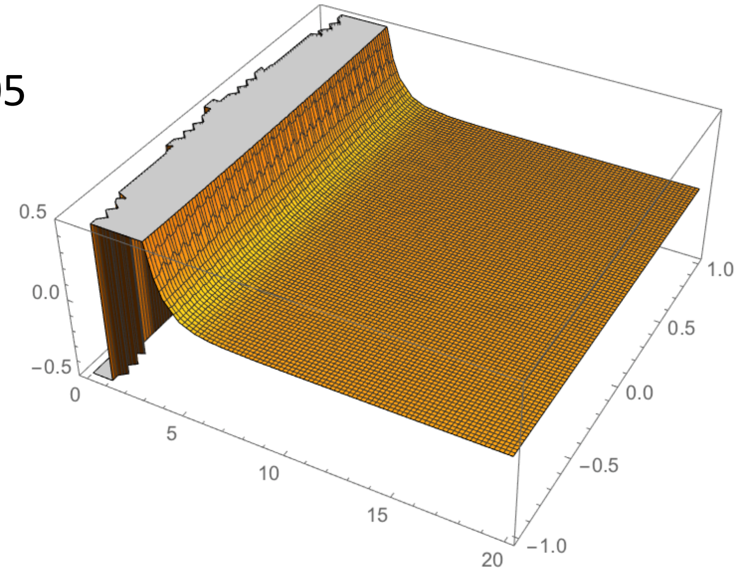

GRO J1655-40
A = 6.3
S = 0.98
Q =0

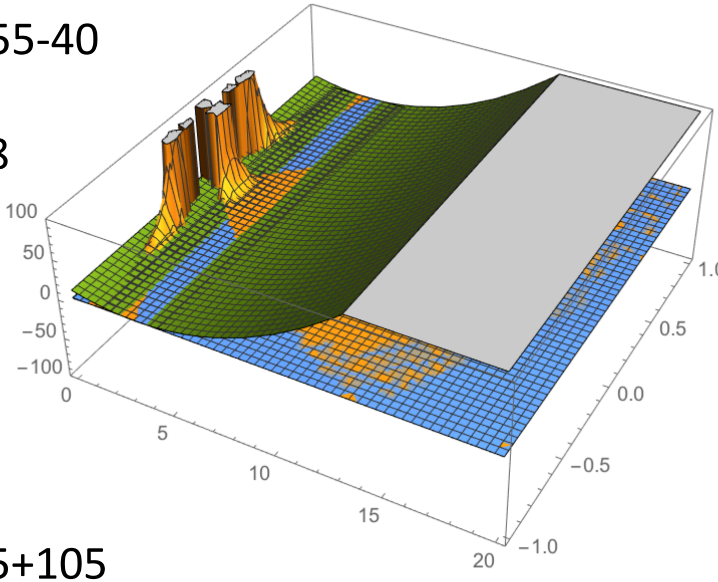

XTE J1550-564
A = 9.6
S = 0.76
Q = 0

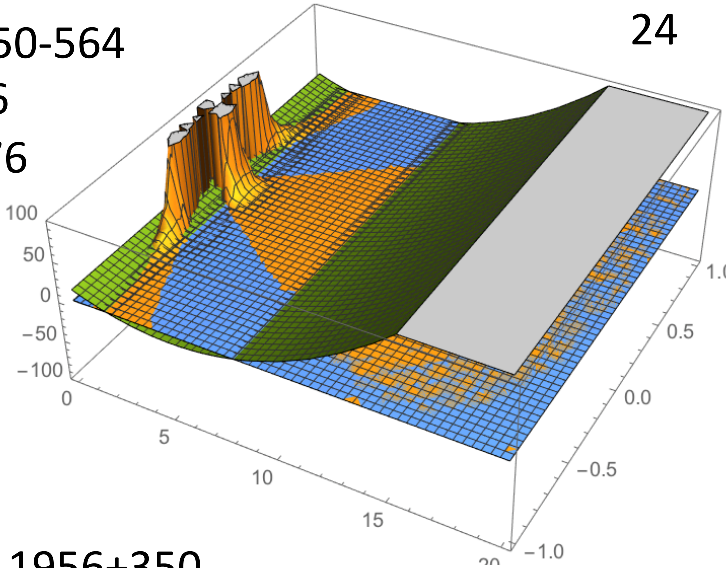

GRS 1915+105
A = 14
S = 0.98
Q =0

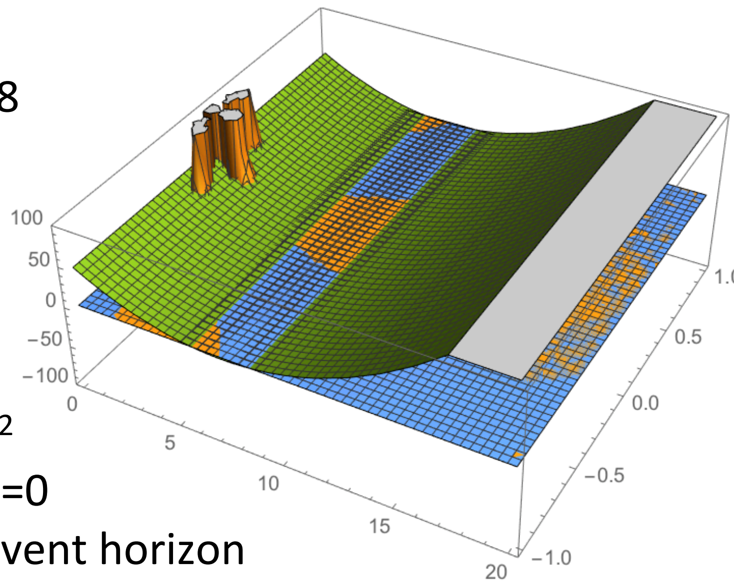

CYG X-1 1956+350
A = 10
S = 0.05
Q =0

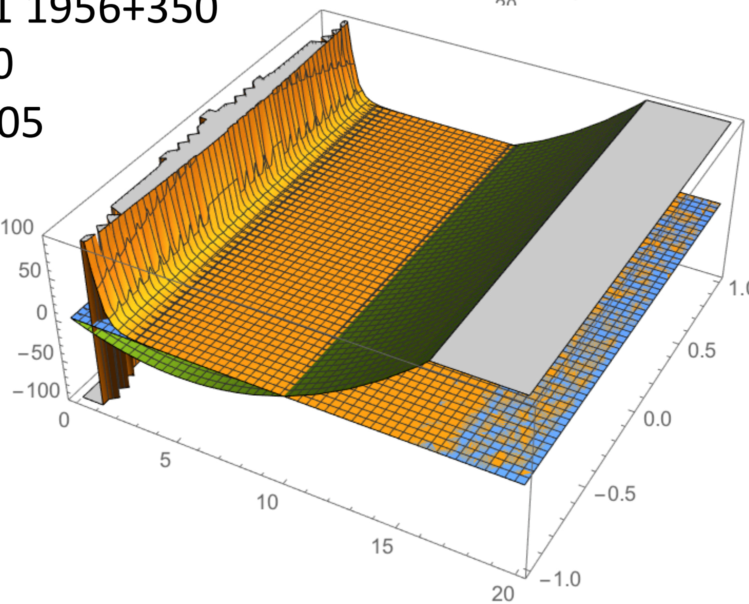

orange: R^2
blue: R=0
Green: event horizon

CONCLUSIONS

1. Basic formalism leading to the Einstein's field equation and some of the exact solutions are introduced. (Schwarzschild metric and Kerr-Newman metric)

2. Kerr metric in Boyer-Lindquist coordinates system has been discussed and graphical presentations of quadratic curvature invariant as well as the event horizon and ergosphere for some of black holes have been given, which were obtained by using **Mathematica** program (ver. 11.3).

3. Further investigation related to this topic would include more detailed analysis on the space-time structure, astrophysical jet, universal magnetic fields and reconnection, worm hole, and so on, as well as the applications to the analysis of observational data.

4. Possible extension of the theory to include the spontaneous magnetic fields in the formalism will be pursued.